


RESEARCH

Open Access



# Suspicious lung lesions for malignancy: the lesion-to-spinal cord signal intensity ratio in T2WI and DWI–MRI versus PET/CT; a prospective pathologic correlated study with accuracy and ROC analyses

Ahmed Samir<sup>1\*</sup> , Heba Abd Elmonsef Abd Elmenem<sup>2</sup>, Adel Rizk<sup>1</sup>, Abdelaziz Elnekeidy<sup>1</sup>, Ayman Ibrahim Baess<sup>3</sup> and Dina Altarawy<sup>1</sup>

## Abstract

**Background** The multi-detector computed tomography (MDCT) and tissue biopsy are the gold standards for the evaluation of lung malignancies. However, there is a wide range of pulmonary indeterminate lesions that could mimic lung cancer. Furthermore, the diagnosis of malignancy could be challenging if the lesion is small and early presenting by a part-solid or ground-glass nodule or if surrounded by parenchymal lung reaction with consolidation and atelectasis. The previous literature focused on the role of diffusion-weighted image–magnetic resonance imaging (DWI) and the apparent diffusion coefficient (ADC) mapping in the evaluation of lung malignancy. A novel quantitative T2 assessment is provided and tested in this study. *Aim of the work:* To evaluate the accuracy of specific non-invasive quantitative magnetic resonance imaging (MRI) parameters in the characterization of suspicious lung lesions and the discrimination between the malignant and benign nature. They included the lesion-to-spinal cord signal intensity ratio in T2-WI and DWI as well as the mean and minimum apparent diffusion coefficient (ADC) values. This is performed using a prospective pathologic correlated study with receiver-operating characteristics (ROC) analysis and comparison with positron emission tomography (PET-CT) accuracy results.

**Results** This study was prospectively performed during the period between June/2021 and June/2022. It was conducted on 43 suspicious lung lesions detected by MDCT. MRI and PET/CT examinations were performed for all patients, and the results were compared to the final diagnosis obtained after biopsy and pathological assessment, using the statistical tests of significance and *P*-value. Cutoff values were automatically calculated, and then, accuracy tests and ROC analyses were performed. Five expert radiologists and a single consulting pulmonologist participated in this study. The inter-rater reliability ranges between good and excellent with the intra-class correlation coefficient (ICC) ranging between 0.85 and 0.94. *In T2-WI: The lesion-to-spinal cord signal intensity ratio* was higher in the malignant group ( $1.35 \pm 0.29$ ) than in the benign group ( $0.88 \pm 0.40$ ), ( $P < 0.001$ ). At the estimated cutoff value ( $> 1$ ), the sensitivity was 96.43%, the specificity was 80.00%, and  $AUC = 0.86$ . *In b500-DWI: The lesion-to-spinal cord signal intensity ratio* was higher in the malignant group (0.70–1.35) than in the benign group (0.20–0.70) ( $P < 0.001$ ). At the estimated cutoff value ( $> 0.7$ ), the sensitivity was 71.43%, the specificity was 86.67%, and  $AUC = 0.86$ . *The mean and minimum ADC*

\*Correspondence:

Ahmed Samir

Sweetjomana36@hotmail.com

Full list of author information is available at the end of the article



© The Author(s) 2023. **Open Access** This article is licensed under a Creative Commons Attribution 4.0 International License, which permits use, sharing, adaptation, distribution and reproduction in any medium or format, as long as you give appropriate credit to the original author(s) and the source, provide a link to the Creative Commons licence, and indicate if changes were made. The images or other third party material in this article are included in the article's Creative Commons licence, unless indicated otherwise in a credit line to the material. If material is not included in the article's Creative Commons licence and your intended use is not permitted by statutory regulation or exceeds the permitted use, you will need to obtain permission directly from the copyright holder. To view a copy of this licence, visit <http://creativecommons.org/licenses/by/4.0/>.

values were lower in the malignant group ( $0.6\text{--}1.3$  and  $0.3\text{--}1.1 \times 10^{-3} \text{ mm}^2/\text{s}$ ) than the benign group ( $1\text{--}1.6$  and  $0.7\text{--}1.4 \times 10^{-3} \text{ mm}^2/\text{s}$ ), ( $P < 0.01$  and  $< 0.001$ , respectively). At their estimated cutoff values ( $\leq 1.2$  and  $\leq 0.9 \times 10^{-3} \text{ mm}^2/\text{s}$ , respectively), the sensitivity was (71.4 and 85.7%), specificity was (83.3 and 66.7%), respectively, and  $\text{AUC} = 0.77$  for both. PET/CT had 96.4% sensitivity, 92.3% specificity, and  $\text{AUC} = 0.94$ .

**Conclusions** PET-CT remains the most specific and sensitive tool for the differentiation between benign and malignant lesions. The lesion-to-cord signal intensity ratios in T2WI and DWI-MRI and to a minor extent the mean and minimum ADC values are also considered good parameters for this differentiation based on their accurate statistical results, particularly if PET/CT was not available or feasible. The study added to the previous literature a novel quantitative T2WI assessment which proved a high sensitivity equal to PET/CT with a lower but a good specificity. The availability, expertise, time factor, and patients' tolerance remain challenging factors for MRI.

**Keywords** Suspicious lung lesions, DWI, MRI, PET

## Background

Multi-detector computed tomography (MDCT) is the gold standard for the evaluation of lung pathologies. However, there is a wide range of pulmonary pseudolesions or equivocal lesions that could mimic lung cancer clinically and radiologically [1]. For example, diseases with fibrosis and parenchymal distortion such as sarcoidosis and progressive massive fibrosis may mimic lung malignancy [2, 3]. Early scar carcinoma on top of pulmonary tuberculosis could also pass unnoticed [4].

On the other hand, other locally malignant and malignant lung lesions may be presented with innocent-looking lesions. For example, the adenocarcinoma in situ (AIS), the minimally invasive (MIA), and the invasive mucinous carcinoma (old termed bronchoalveolar carcinoma BAC) could be presented by either pure, part-solid, or solid lung nodules [5, 6]. Lung carcinoid is a central peri-bronchial tumor with small endo-bronchial budding that presents with hemoptysis. It could be equivocal in CT examinations when small or give false negative results in PET/CT examinations [7].

The high-quality lung MRI can contribute to evaluating numerous pulmonary diseases including lung cancer and malignant pleural tumors. Similar to CT, proton MRI can reveal structural evaluation concerning mucus distribution, bronchiectasis, inflammatory airway wall thickening, consolidation, and atelectasis [8]. It has also the advantage of the lack of ionizing irradiation, particularly in patients who require frequent follow-up examinations [9].

Additionally, the T2-weighted images provide good lesion-to-background contrast. The healthy lung has no signal, so high sensitivity is achieved in the detection of lung infiltrates, atelectasis, and solid lesions [10]. The DWI-MRI can be also used in lung examination and gives promising results in differentiation between malignant and benign pulmonary lesions [11]. Qualitatively, it can delineate the parenchymal lesions from the adjacent pleura and mediastinum [12]. Quantitatively, it also

provides the ADC value in addition to signal intensity (SI)-related parameters such as lesion-to-spinal cord signal intensity ratio [13].

The previous literature focused on the role of diffusion-weighted image-magnetic resonance imaging (DWI) and apparent diffusion coefficient (ADC) mapping in the evaluation of lung malignancy. A novel quantitative T2 assessment is furtherly provided and tested in this study.

*Aim of the work:* To evaluate the accuracy of specific non-invasive quantitative magnetic resonance imaging (MRI) parameters in the characterization of suspicious lung lesions and the discrimination between the malignant and benign nature. They included the lesion-to-spinal cord signal intensity ratio in T2-WI and DWI as well as the mean and minimum apparent diffusion coefficient (ADC) values. This is performed using a prospective pathologic correlated study with receiver-operating characteristics (ROC) analysis and comparison with positron emission tomography (PET-CT) accuracy results.

## Methods

A flow diagram (Fig. 1) is provided to demonstrate the study design, methodology, steps, and brief results.

This study was prospectively performed during the period between June/2021 and June/2022. It was conducted on 43 suspicious lung lesions detected by MDCT. MRI and PET/CT examinations were performed for all patients, and the results were compared to the final diagnosis obtained after biopsy and pathological assessment, using the statistical tests of significance and  $P$ -value. Statistical cutoff values were automatically calculated, and then, accuracy tests and ROC analyses were performed.

The inclusion criteria were as follows: (1) Suspicious lung nodules or masses in chest CT having speculated outlines and/or desmoplastic reaction (17 lesions, including four solitary pulmonary nodules), (2) Suspicious atypical pulmonary consolidations in chest CT showing interrupted or absent air bronchogram (ten lesions), (3) Suspicious fibrotic lesions or scarring in

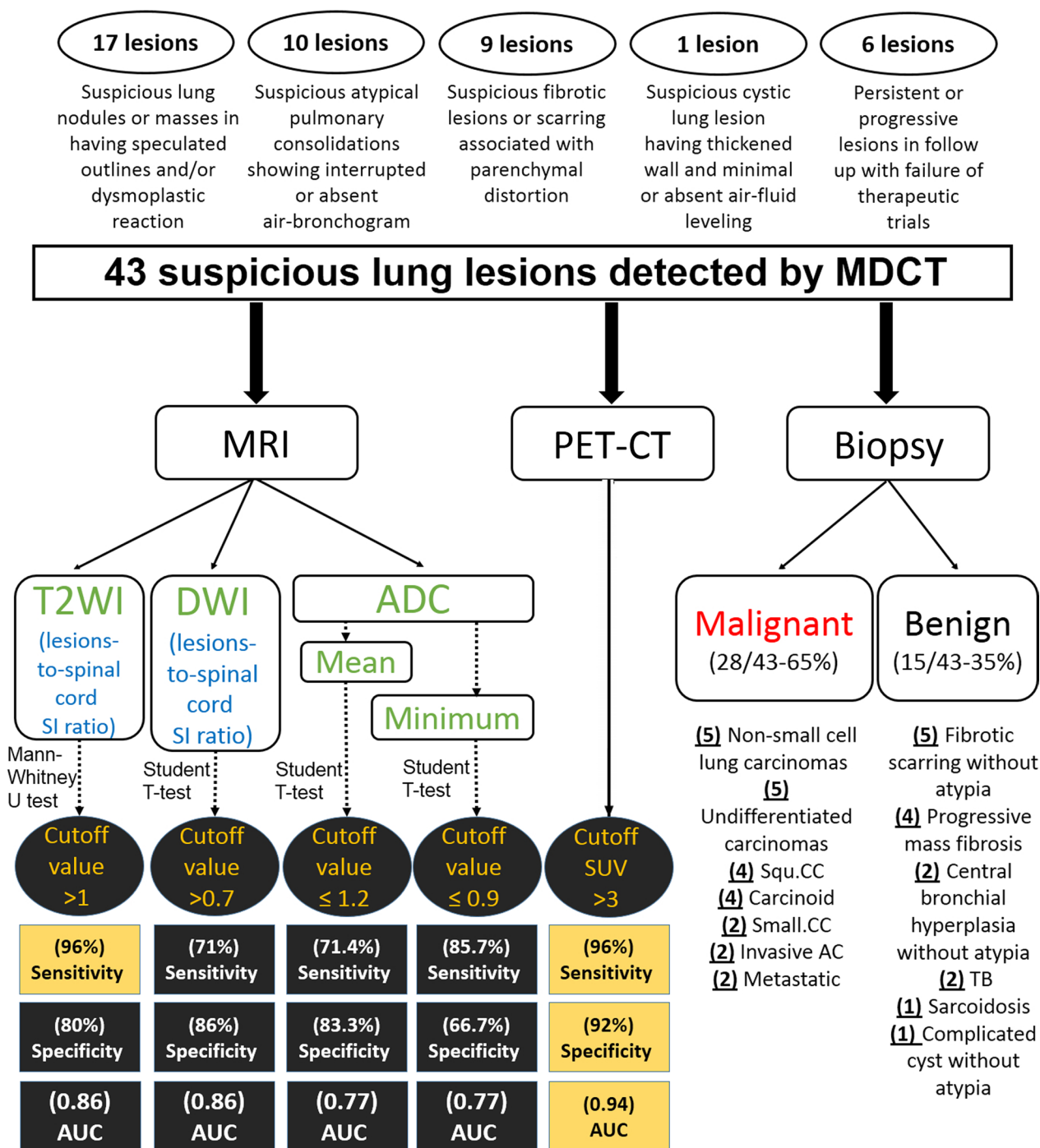


Fig. 1 A flow diagram is demonstrating the study design, methodology, and brief results

chest CT associated with parenchymal distortion (nine lesions), (4) Suspicious cystic lung lesions in chest CT having thickened wall and minimum or absent air-fluid leveling (one lesion), (5) Persistent or progressive lesions in chest CT examination with failure of therapeutic trials (six lesions).

The exclusion criteria were as follows: (1) Densely calcific lesions in chest CT, (2) Contraindications for MRI or PET/CT application, (3) Poor quality of images and artifacts because of patients' tachypnea, (4) Absent pathological confirmation, and finally (5) Patients who refused to give an ethical consent.

The study was approved by the "Institutional Ethics Committee" [IRB No: (00012098), FWA No: (00018699)]. Written informed consent was obtained from every patient. This manuscript does not overlap with any previously published works.

Five expert radiologists participated in this study. Their experience ranged from 7 to 36 years. They worked independently and were blinded by the clinical data. A single consulting pulmonologist with 22 years of experience shared also in this study.

**MRI scanning and sequences**

Respiratory gated closed 1.5 T MRI examinations were performed on either PHILIPS Achieva (Netherlands) or TOSHIBA titan (Japan) scanners. The following MRI spin echo sequences were applied without IV contrast administration:

- A. T1WI (axial and coronal): the repetition time/echo time=10/5 ms, the slice thickness=5 mm, the gap=0.5 mm, and the field of view=35–40 cm.
- B. T2WI (axial and coronal): the repetition time/echo time=665/80 ms, the slice thickness=5 mm, the gap=1.5 mm, and the field of view=35–40 cm.
- C. Axial DWI was acquired at intermediate to high *b* value (500–800–1000 s/mm<sup>2</sup>) with 4–9 slice thickness and 0.5–1.5 mm interslice gap.

- D. ADC mapping using single-shot echo-planar spin-echo sequences.

**MRI qualitative and quantitative assessment**

The "OsiriX MD 11.0" software (Pixmeo SARL, Geneva, Switzerland) and the "Radiant" dicom viewer were utilized for imaging review.

The qualitative assessment of the lesions was performed in the T2WI, DWI, and ADC mapping. The lesions with high T2 signal intensity are considered suspicious in comparison to fibrotic lesions with low T2 signal intensity. Extra-pleural space, mediastinal or vascular invasions were carefully observed. The diffusion restriction was determined by the bright signal in the DWI and the low signal in the ADC mapping.

Three quantitative parameters were utilized in this study, as follows:

- (1) The lesion-to-spinal cord signal intensity ratio in T2WI (novel procedure): Two ROIs were placed: one over the center of the lesion (excluding necrotic or calcific core) and the other over the spinal cord in T2WI at the same slice. Recording of the signal intensities was repeated twice by each of two independent expert radiologists, and average values were taken and divided to give the ratio (Table 1).

**Table 1** Inter-rater reliability and intra-class correlation coefficient (ICC)

	No.	1st group reading	2nd group reading	P-value	ICC	95% CI	Level of agreement
T2WI based L-to-SC SI ratio							
Malignant	28	1.35 ± 0.29	1.32 ± 0.31	< 0.001*	0.899	0.794–0.952	Good
Benign	15	0.88 ± 0.40	0.89 ± 0.33	< 0.001*	0.941	0.833–0.980	Excellent
Overall	43	1.19 ± 0.40	1.17 ± 0.37	< 0.001*	0.942	0.896–0.968	Excellent
b500-DWI based L-to-SC SI ratio							
Malignant	28	1.05 ± 0.41	1.08 ± 0.37	< 0.001*	0.922	0.840–0.963	Excellent
Benign	15	0.48 ± 0.30	0.50 ± 0.24	< 0.001*	0.911	0.760–0.969	Excellent
Overall	43	0.85 ± 0.46	0.88 ± 0.43	< 0.001*	0.950	0.909–0.972	Excellent
Mean ADC value in 10 <sup>-3</sup> mm <sup>2</sup> /s							
Malignant	28	1.10 ± 0.27	1.15 ± 0.32	< 0.001*	0.845	0.711–0.915	Good
Benign	15	1.19 ± 0.26	1.23 ± 0.32	< 0.001*	0.890	0.729–0.958	Good
Overall	43	1.13 ± 0.29	1.18 ± 0.32	< 0.001*	0.861	0.760–0.927	Good
Minimum ADC value in 10 <sup>-3</sup> mm <sup>2</sup> /s							
Malignant	28	0.80 ± 0.29	0.85 ± 0.33	< 0.001*	0.851	0.705–0.928	Good
Benign	15	0.89 ± 0.28	0.93 ± 0.31	< 0.001*	0.897	0.727–0.964	Good
Overall	43	0.83 ± 0.29	0.88 ± 0.32	< 0.001*	0.865	0.762–0.925	Good

L-to-SC SI ratio Lesion-to-spinal cord signal intensity ratio

CI Confidence interval

Data were expressed using mean ± SD (standard deviation)

\*Statistically significant at P-value ≤ 0.05

- (2) The lesion-to-spinal cord signal intensity ratio in intermediate to high DWI: Two ROIs were placed: one over the center of the lesion (excluding necrotic or calcific core) and the other over the spinal cord in DWI at the same slice. Again, recording of the signal intensities was repeated twice by each of two independent expert radiologists and average values were taken and divided to give the ratio (Table 1).
- (3) The mean and minimum ADC values were calculated using a wide region of interest (ROI) over the center of the lesion which showed the most diffusion restriction excluding necrotic areas, foci of calcifications, and peripheral areas of lung consolidations or collapse. This step was also repeated twice by each of two independent expert radiologists, and the average of each value was then calculated and used as the estimated value (Table 1).

N.B: The ROI sizes over the lesions were standardized and equal to that over the spinal cord at the same level in cases of pulmonary nodular lesions (<3 cm) [13], but they differed in cases of lung consolidations or masses; according to the size of their solid components, they were widened as much to involve the solid restricting components and exclude the necrotic changes.

#### PET/CT examinations

All patients performed PET/CT examinations on a hybrid PET/CT scanner (Siemens Biograph 64 PET/CT scanner, Germany). The following routine precautions and preparation steps were respected: (1) Fasting except for water and avoiding heavy muscular exercises were instructed six hours before the examinations, (2) Voiding of urine was instructed before the examination, (3) The blood sugar level should be less than 150 mg/dl, and (4) Patients were instructed to stop talking during the examination. 18-FDG was injected at a rate of around 5MBg/kg body weight. The above 3 standardized uptake values (SUV) are universally utilized as a cutoff value of malignancy.

#### Clinical contribution

A full clinical examination and laboratory profile were performed. Either bronchoscopic-guided or open lung biopsy was taken. Finally, the tissue pathological diagnosis was encountered and compared with the clinical and radiological data.

#### Reference and statistical analyses (in order)

- (1) The inter-observer agreement or inter-rater reliability between two expert consulting radiologists was

estimated using an online calculator "<https://www.raterreliability.com/>" and the intra-class correlation coefficient (ICC) was calculated.

- (2) IBM SPSS software package version 20.0. (Armonk, NY: IBM Corp) was utilized. The quantitative data were described using the range (minimum and maximum), the mean, the standard deviation, the median, and the interquartile range (IQR). After the comparison with the final diagnosis obtained by pathological assessment, the significance of the obtained results was judged using the Chi-square test at  $P$  value < 0.05.
- (3) Mann–Whitney  $U$  test compared T2WI lesion-to-spinal cord SI ratio and estimated the cutoff value according to Youden index.
- (4) Student  $T$ -test compared the DWI lesion-to-spinal cord SI ratio, evaluated the mean and minimum ADC values, and estimated the cutoff values.
- (5) Accuracy tests were then performed. They included the sensitivity, the specificity, and the positive and negative predictive values.
- (6) ROC analysis using the "QI Macros" system evaluated the diagnostic role of T2WI and DWI in the differentiation of benign and malignant lesions.

## Results

### Demographic features, clinical data, and final pathologically proven diagnoses

The male-to-female ratio in the included patients was 76%:24%. Their age ranged from 24 to 80 years while their mean age was  $56 \pm 17$  SD years. Smoking history was positive in 37% of patients, and history of distant malignancy was only positive in two patients. All patients complained of cough, while 80% complained of dyspnea, 60% complained of chest pain, and 20% complained of hemoptysis.

The included lung nodules ranged between 1.6 and 3 cm in diameter; meanwhile, the lung consolidations and masses reached 7 cm in size. The upper-to-lower lobar lung involvement ratio was 60%:40%.

28/43 (65%) lesions were pathologically proved with malignancy (Fig. 1), including five non-small cell lung carcinomas (Fig. 2), five undifferentiated carcinomas, four squamous cell carcinomas, four large cell lymphomas (Fig. 3), four carcinoid tumors (Fig. 4), two small cell carcinomas (Fig. 5), two invasive adenocarcinomas, and two metastatic lesions (Fig. 6).

15/43 (35%) lesions were pathologically proved to be benign (Fig. 1) as follows: Fibrotic scarring without atypia was proved in five lesions. Progressive mass fibrosis was proved in four lesions (Fig. 7). Central bronchial



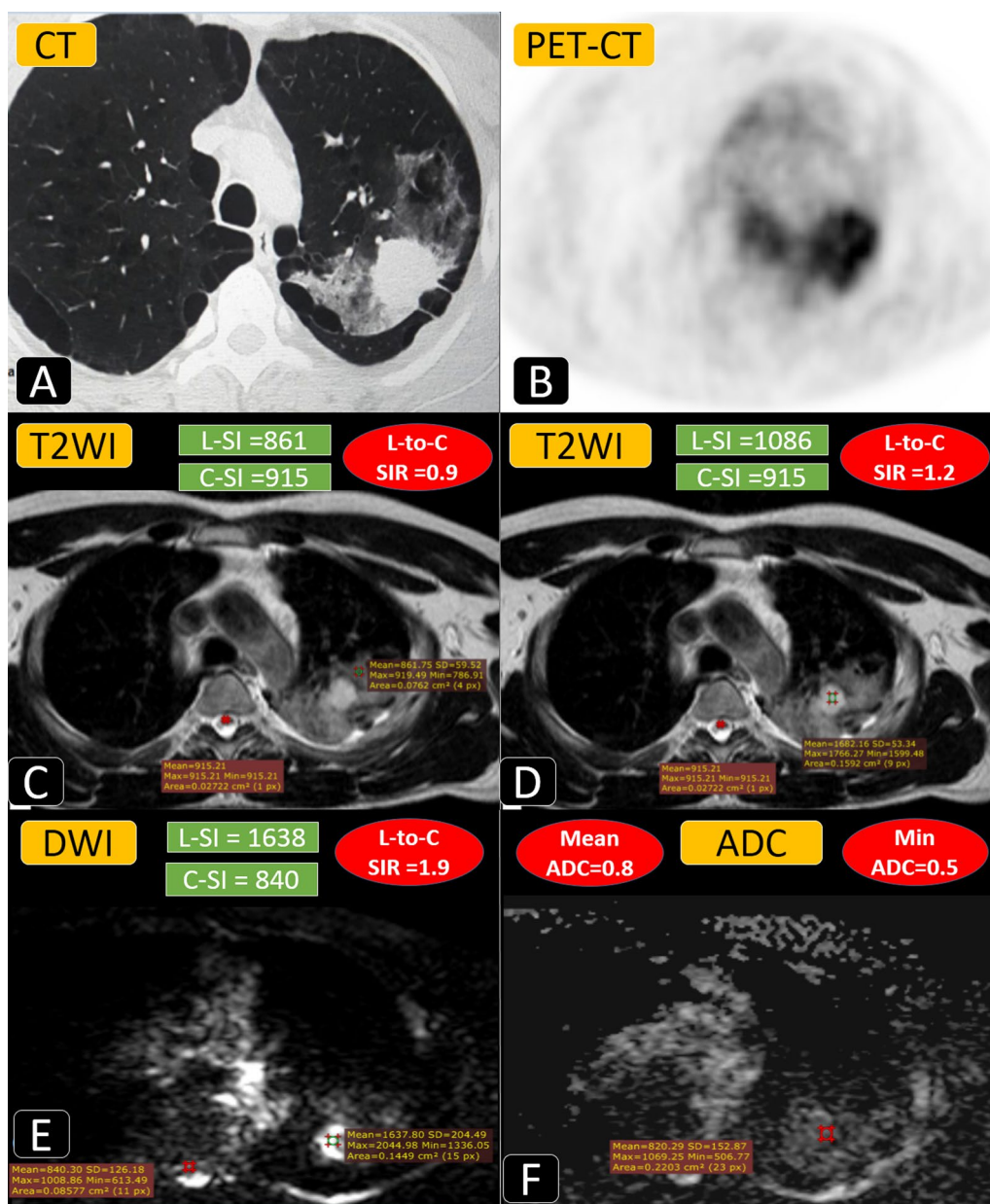


**Fig. 2** A 50-year-old male patient complained of chronic cough and chest pain. **A** Axial chest CT cut (lung window) showed left upper lobar apical-posterior large sub-pleural homogeneous solid lung nodule showing two pleura tags and surrounded by parenchymal ground-glass reaction/halo; this is on a background of bilateral upper lobar para-septal emphysema. **B** Axial chest PET-CT image showing high 18F-FDG uptake. **C** Axial T2WI shows the high signal intensity of the nodule. After placing two ROIs within the nodule and the spinal cord, the lesion-to-spinal cord signal intensity ratio was calculated = 0.9. **D** Same axial T2WI showing iso-intensity signal of the surrounding lung parenchyma. After placing two ROIs within the parenchyma around the lesion and the spinal cord, the lesion-to-spinal cord signal intensity ratio was calculated = 1.2. **E** Axial DWI showing bright signal of restricted diffusion and lesion-to-spinal cord signal intensity ratio was calculated = 1.9. **F** ADC mapping images showing low signal intensity with minimum ADC =  $0.5 \times 10^{-3}$  mm<sup>2</sup>/s and mean ADC =  $0.8 \times 10^{-3}$  mm<sup>2</sup>/s. Referring to the estimated cutoff values, T2WI L-to-SC SI ratio, DWI L-to-SC SI ratio, minimum ADC, and mean ADC suggested a malignant process. Pathologically proven non-small cell lung cancer (NSCLC)

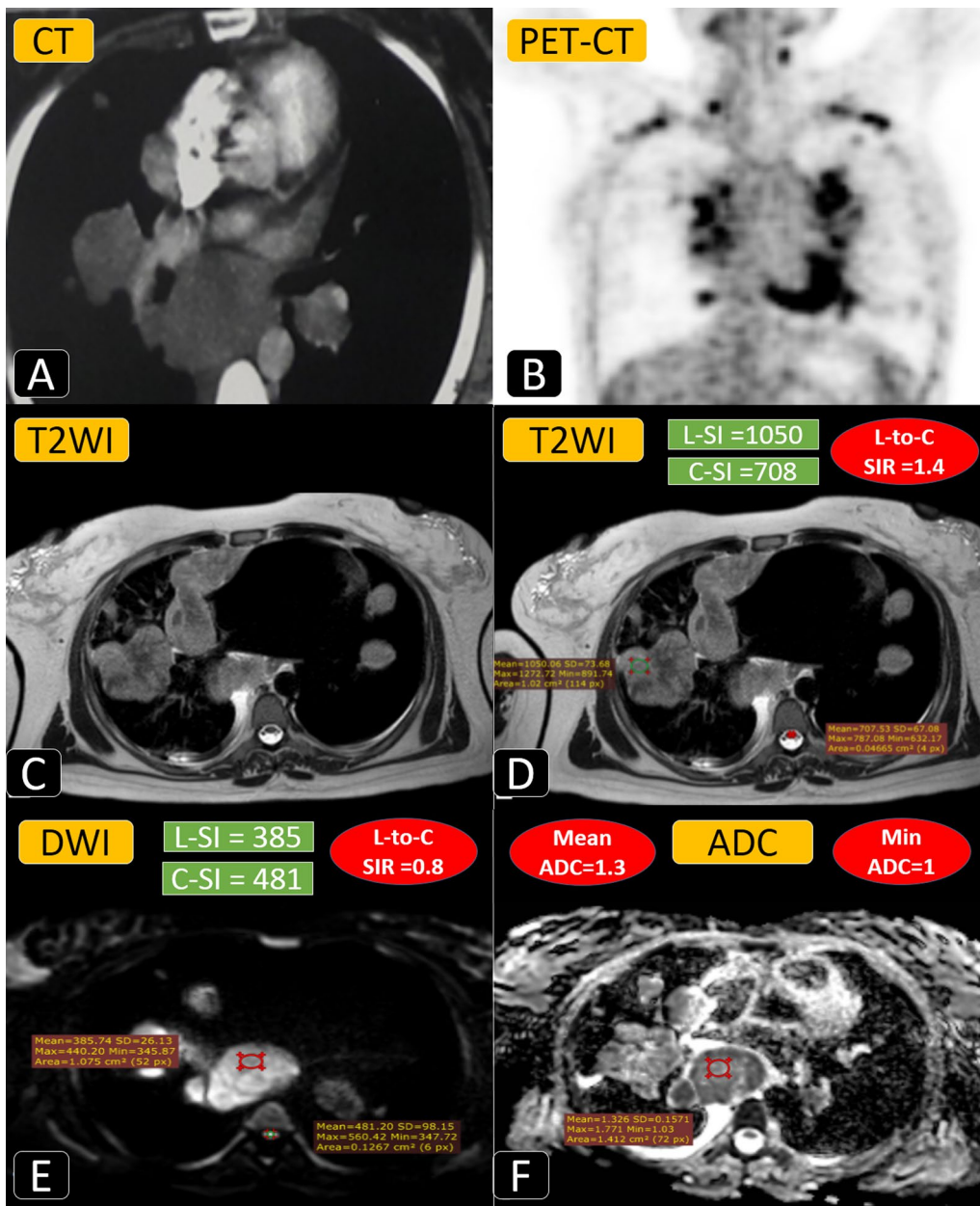


**Fig. 3** A 24-year-old female patient complained of chronic cough and dyspnea. **A** Axial contrast-enhanced chest CT cut (mediastinal window) showed bilateral hilar and posterior mediastinal sub-carinal nodal enlargement. **B** Coronal chest PET-CT image showing high 18F-FDG uptake at thoracic, bilateral supra-clavicular, and left cervical nodal enlargement. **C, D** Axial T2WI showing the high signal intensity of bilateral nodal and parenchymal masses. After placing two ROIs within the largest lesion and the spinal cord, the lesion-to-spinal cord signal intensity ratio was calculated = 1.4. **E** Axial DWI showing bright signal of restricted diffusion and lesion-to-spinal cord signal intensity ratio was calculated = 0.8. **F** ADC mapping images showing low signal intensity with minimum ADC ( $1 \times 10^{-3} \text{ mm}^2/\text{s}$ ) and mean ADC ( $1.3 \times 10^{-3} \text{ mm}^2/\text{s}$ ). Referring to the estimated cutoff values, T2WI L-to-SC SI ratio, DWI L-to-SC SI ratio, minimum ADC, and mean ADC suggested a malignant process. Pathologically proven large cell lymphoma

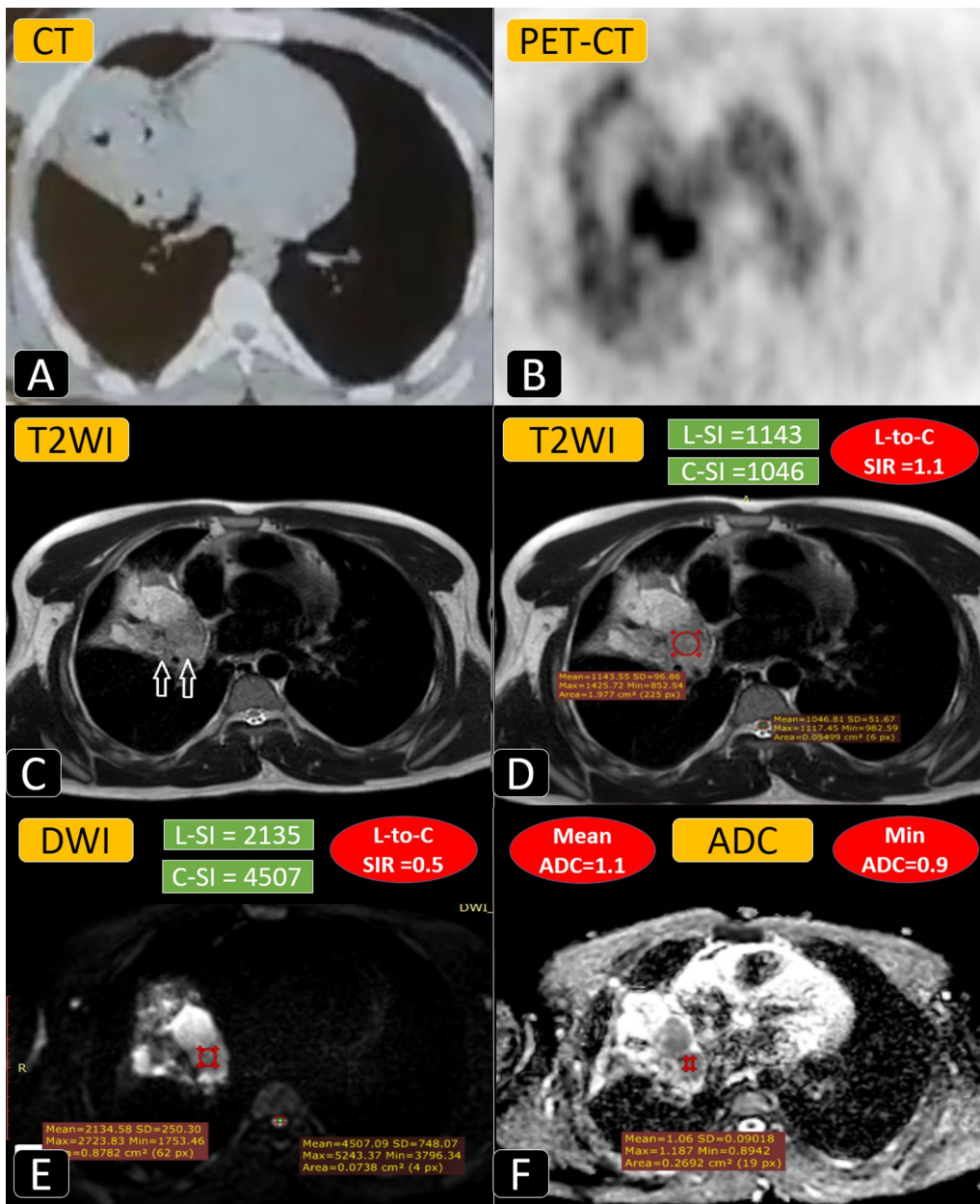


**Fig. 4** A 30-year-old male patient complained of chest pain, dyspnea, and hemoptysis. **A** Axial chest CT cut (mediastinal window) showed right middle lobar consolidation collapse with interrupted air bronchogram and suspected iso-dense central obstructing lesion. **B** Axial chest PET-CT image showing high 18F-FDG uptake at the right peri-hilar lesion. **C, D** Axial T2WI showing the heterogeneous high signal intensity of central obstructing lesion with distal atelectasis. After placing two ROIs within the largest lesion and the spinal cord, the lesion-to-spinal cord signal intensity ratio was calculated = 1.1. **E** Axial DWI showing bright signal of restricted diffusion and lesion-to-spinal cord signal intensity ratio was calculated = 0.5. **F** ADC mapping images showing low signal intensity with minimum ADC ( $0.9 \times 10^{-3} \text{ mm}^2/\text{s}$ ) and mean ADC ( $1.1 \times 10^{-3} \text{ mm}^2/\text{s}$ ). Referring to the estimated cutoff values, the T2WI L-to-SC SI ratio, minimum ADC, and mean ADC suggested a malignant process; however, the DWI L-to-SC SI ratio was mismatched. Pathologically proven carcinoid neoplasm



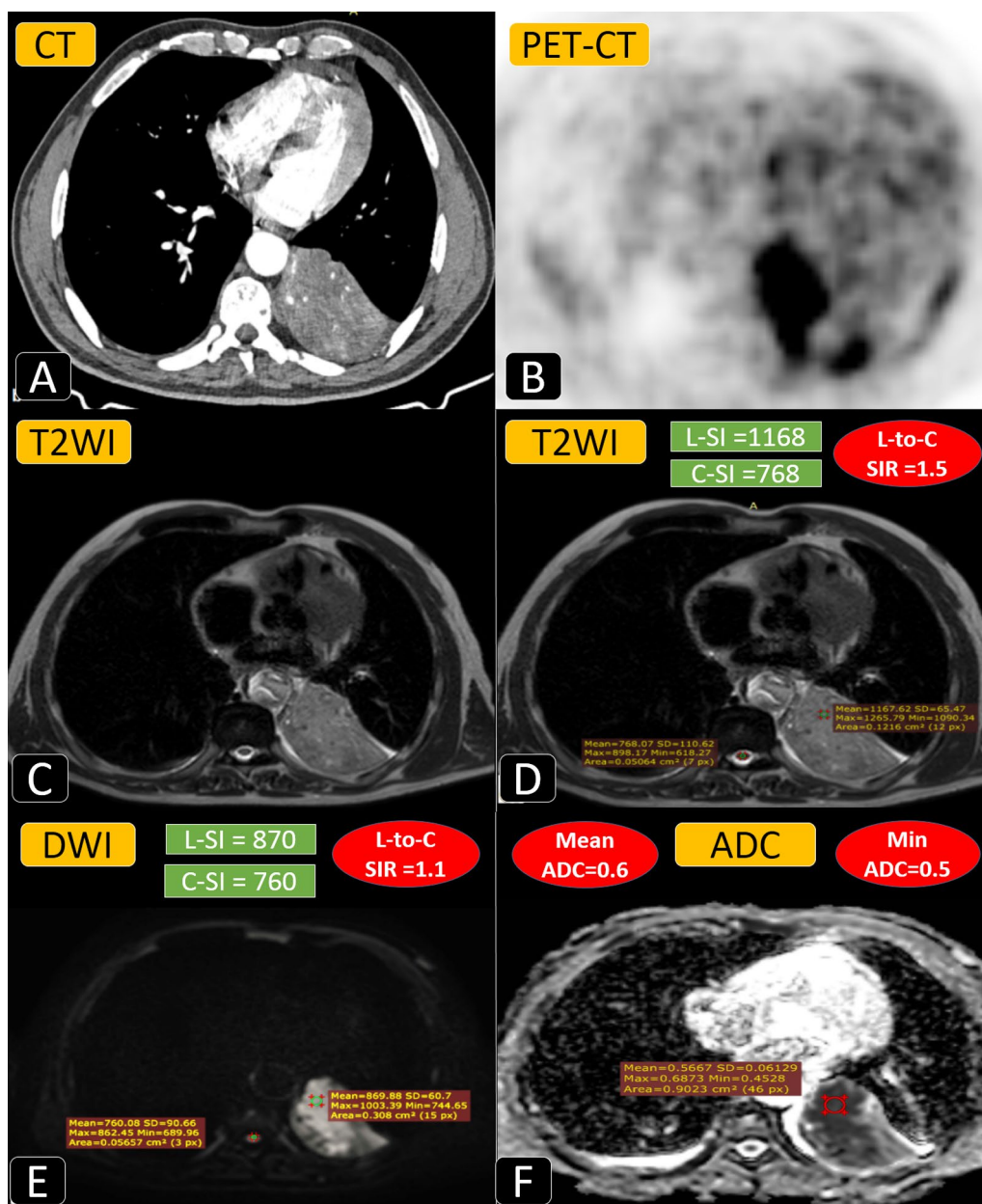


**Fig. 5** A 76-year-old male patient complained of hemoptysis and dyspnea. **A** Axial contrast-enhanced chest CT cut (mediastinal window) showed left medial basal consolidation collapse with internal CT-angiogram and absent air bronchogram with a suspected iso-dense mass lesion. **B** Axial chest PET-CT image showing high 18F-FDG uptake at most of the lesion. **C, D** Axial T2WI shows the high signal intensity of the lesion. After placing two ROIs within the largest lesion and the spinal cord, the lesion-to-spinal cord signal intensity ratio was calculated = 1.5. **E** Axial DWI showing bright signal of restricted diffusion and lesion-to-spinal cord signal intensity ratio was calculated = 1.1. **F** ADC mapping images showing low signal intensity with minimum ADC ( $0.5 \times 10^{-3} \text{ mm}^2/\text{s}$ ) and mean ADC ( $0.6 \times 10^{-3} \text{ mm}^2/\text{s}$ ). Referring to the estimated cutoff values, T2WI L-to-SC SI ratio, DWI L-to-SC SI ratio, minimum ADC, and mean ADC suggested a malignant process. Pathologically proven small cell lung cancer (SCLC)

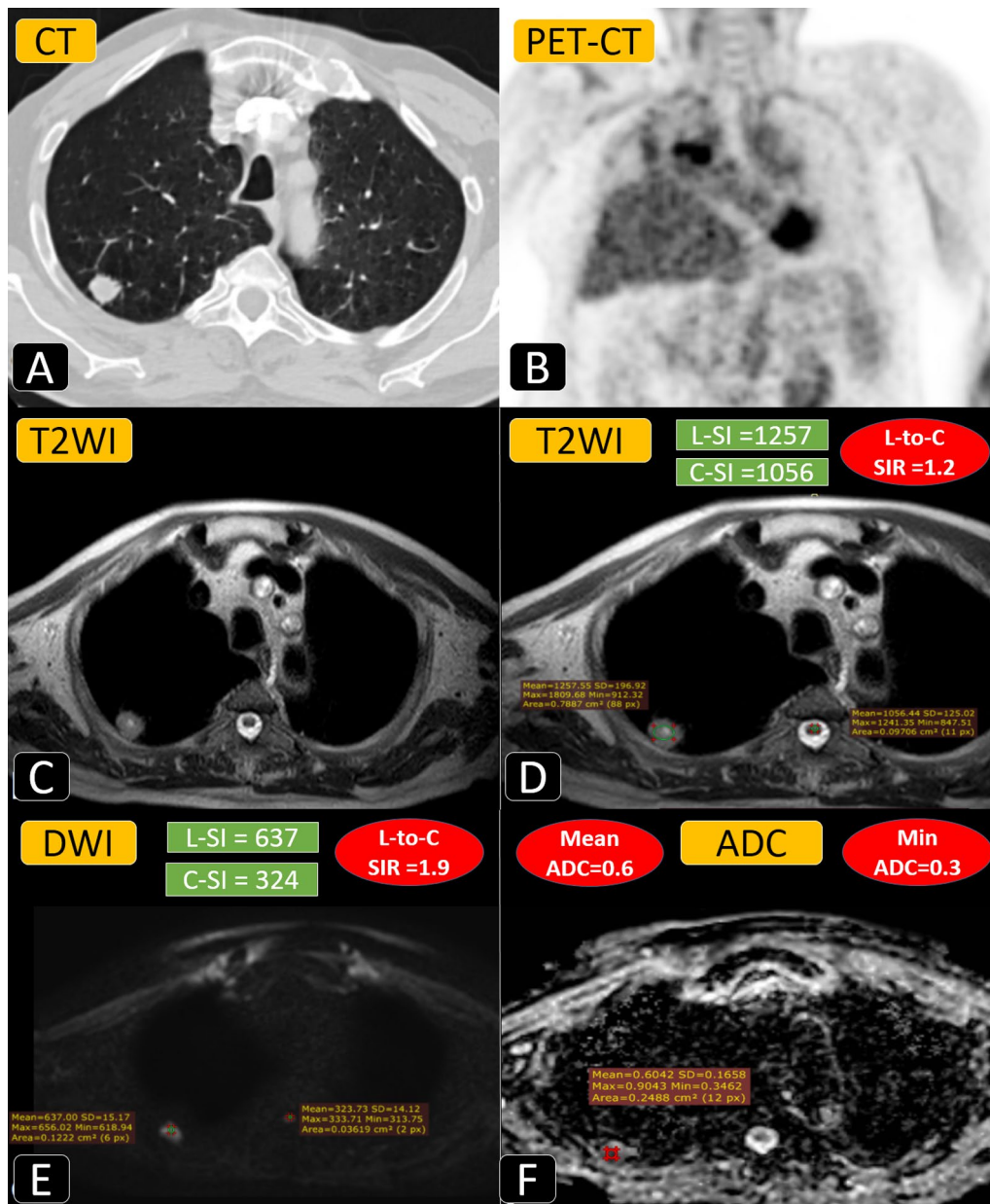


**Fig. 6** A 67-year-old male patient with a history of primary hemangiopericytoma complained of chronic cough. **A** Axial chest CT cut (lung window) showed solitary right upper lobar posterior segmental sub-pleural solid homogeneous lung nodule showing minimum speculated outlines and faint pleural tag. **B** Coronal chest PET-CT image showing high 18F-FDG uptake at the right upper lobar nodular lesion. **C, D** Axial T2WI showing the iso-to-high signal intensity of the lesion. After placing two ROIs within the largest lesion and the spinal cord, the lesion-to-spinal cord signal intensity ratio was calculated = 1.2. **E** Axial DWI showing bright signal of restricted diffusion and lesion-to-spinal cord signal intensity ratio was calculated = 1.9. **F** ADC mapping images showing low signal intensity with minimum ADC ( $0.3 \times 10^{-3} \text{ mm}^2/\text{s}$ ) and mean ADC ( $0.6 \times 10^{-3} \text{ mm}^2/\text{s}$ ). Referring to the estimated cutoff values, T2WI L-to-SC SI ratio, DWI L-to-SC SI ratio, minimum ADC, and mean ADC suggested a malignant process. Pathologically proven solitary metastatic lung deposit

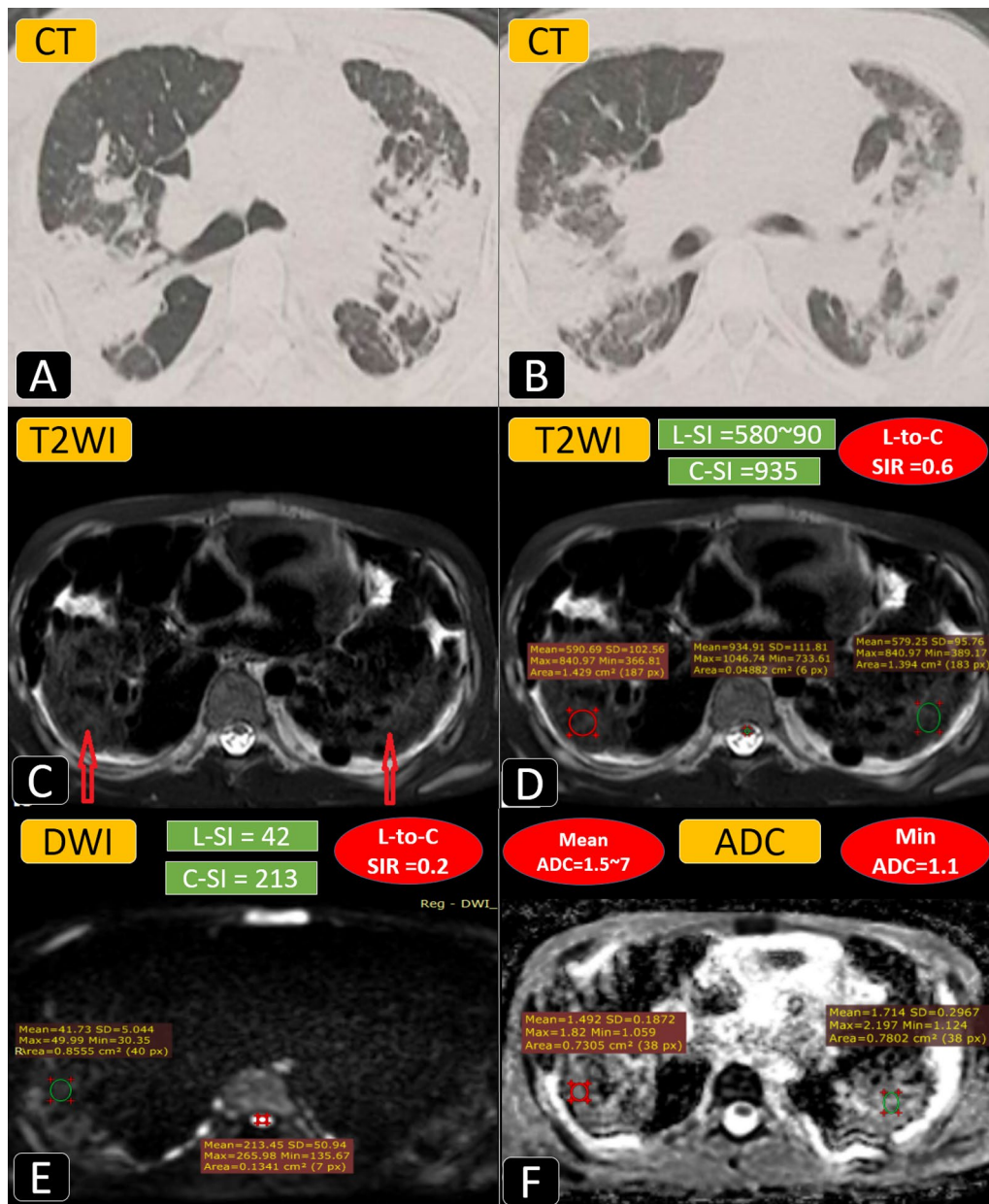


**Fig. 7** A 22-year-old male patient with occupational history correlated with the glass industry complained of chronic cough. **A, B** Axial chest CT cuts (lung window) showed bilateral peri-hilar and peripheral sub-pleural large consolidative mass-like lesions without smooth air bronchogram. **C, D** Axial T2WI showing the low signal intensity of the bilateral large confluent lesions. After placing two ROIs within the largest lesion and the spinal cord, the lesion-to-spinal cord signal intensity ratio was calculated = 0.6. **E** Axial DWI showing low signal intensity denoting non-restricted diffusion and lesion-to-spinal cord signal intensity ratio was calculated = 0.2. **F** ADC mapping images showing low signal intensity with minimum ADC ( $1.1 \times 10^{-3}$  mm<sup>2</sup>/s) and mean ADC ( $1.5-1.7 \times 10^{-3}$  mm<sup>2</sup>/s). Referring to the estimated cutoff values, T2WI L-to-SC SI ratio, DWI L-to-SC SI ratio, minimum ADC, and mean ADC suggested a benign process. Pathologically proven progressive massive fibrosis sequel to pneumoconiosis. PET/CT result was negative



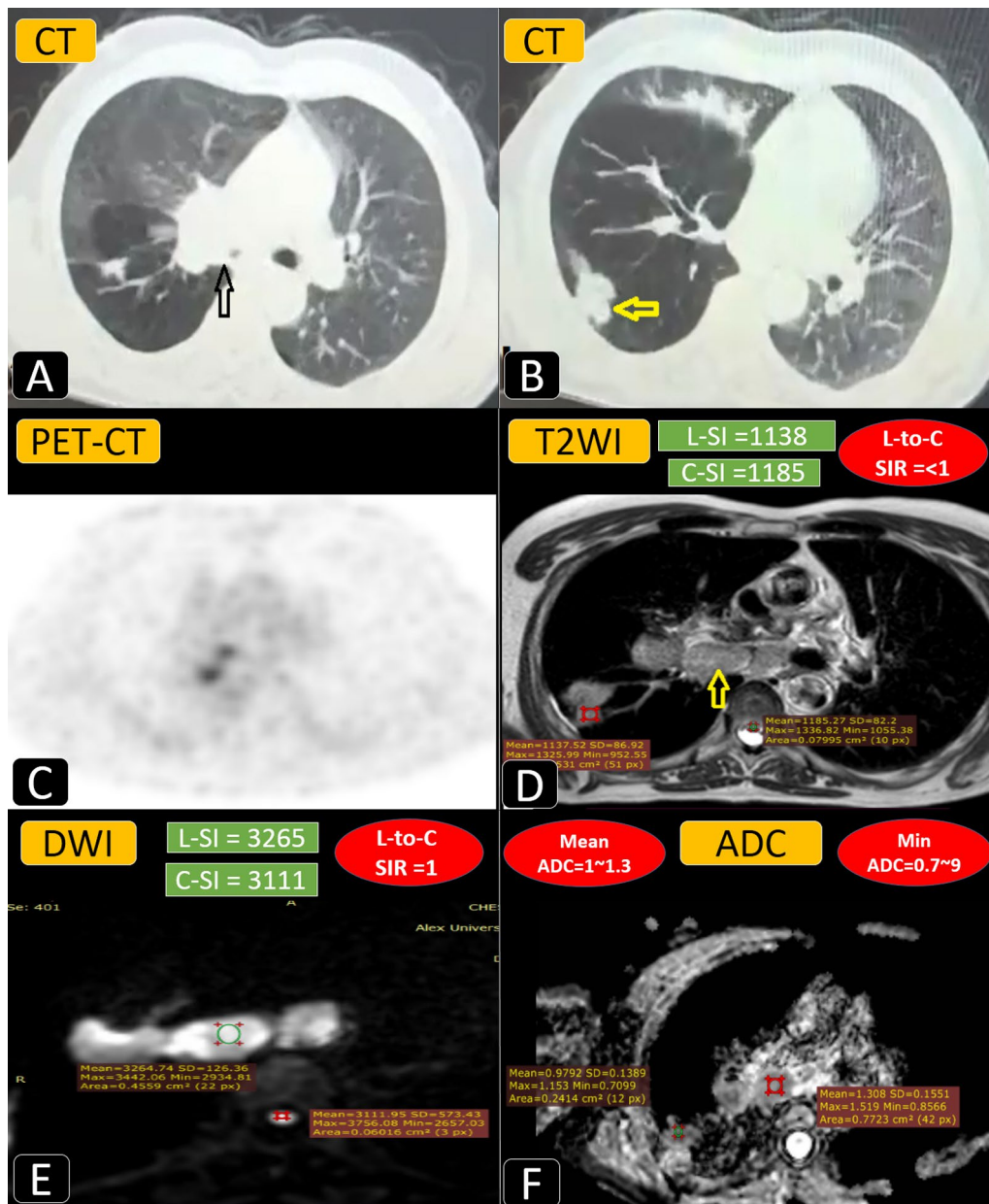


**Fig. 8** A 69-year-old male patient complained of dyspnea. **A, B** Axial chest CT cuts (lung window) showed a right main endo-bronchial lesion attenuating the lumen of the right main bronchus with distal air trapping and the peripheral sub-pleural solid lesion was also noticed. **C** Axial chest PET-CT image showed minimum 18F-FDG uptake. **D** Axial T2WI showing iso-intense signal of the central and peripheral lesions. After placing two ROIs within the peripheral lesion and the spinal cord, the lesion-to-spinal cord signal intensity ratio was calculated = 0.96. **E** Axial DWI showing bright signal denoting restricted diffusion and lesion-to-spinal cord signal intensity ratio was calculated = 1. **F** ADC mapping images showing low signal intensity with minimum ADC ( $0.7\text{--}0.9 \times 10^{-3} \text{ mm}^2/\text{s}$ ) and mean ADC ( $1\text{--}1.3 \times 10^{-3} \text{ mm}^2/\text{s}$ ). Referring to the estimated cutoff values, DWI L-to-SC SI ratio, minimum ADC, and mean ADC suggested a malignant process except for the T2WI L-to-SC SI ratio which suggested a benign nature. Pathologically proven central bronchial hyperplasia without atypia and peripheral benign nodule. (Example for truly positive T2WI ratio and false positive DWI and PET-CT)



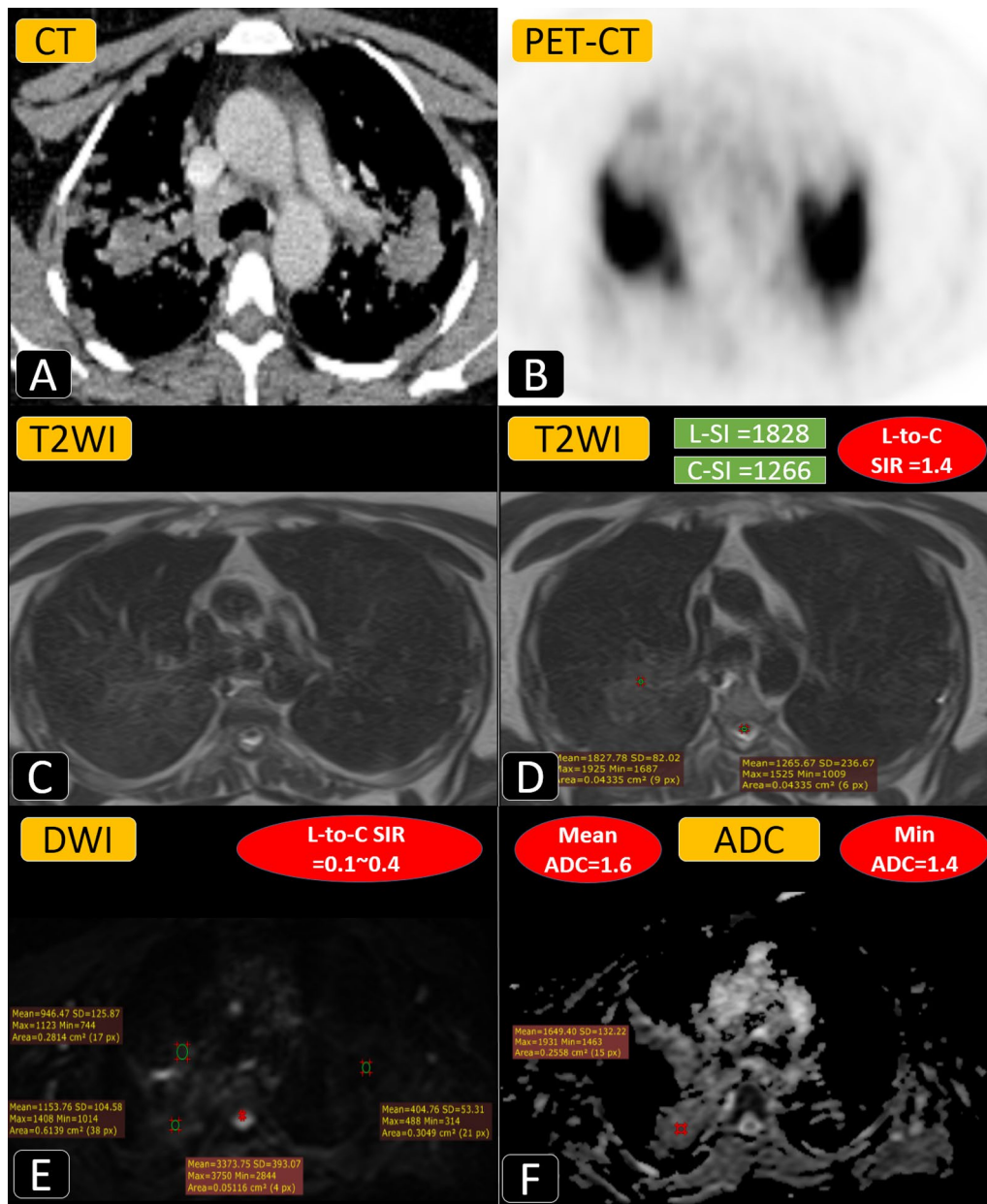


**Fig. 9** A 25-year-old male patient complained of chronic cough and dyspnea. **A** Axial contrast-enhanced chest CT cut (mediastinal window) showed bilateral upper lobar peri-hilar lung masses and scattered peripheral lung nodules. **B** Axial chest PET-CT image showing high bilateral 18F-FDG uptake. **C, D** Axial T2WI shows the low signal intensity of the lesion. After placing two ROIs within the largest lesion and the spinal cord, the lesion-to-spinal cord signal intensity ratio was calculated = 1.4. **E** Axial DWI showing low signal intensity denoting non-restricted diffusion and lesion-to-spinal cord signal intensity ratio was calculated = 0.1–0.4. **F** ADC mapping images showing low signal intensity with minimum ADC ( $1.4 \times 10^{-3} \text{ mm}^2/\text{s}$ ) and mean ADC ( $1.6 \times 10^{-3} \text{ mm}^2/\text{s}$ ). Referring to the estimated cutoff values, only the T2WI L-to-SC SI ratio concerned malignant nature; meanwhile, the DWI L-to-SC SI ratio, minimum ADC, and mean ADC suggested a benign process. Pathologically proven fibrosing parenchymal sarcoidosis. (Example for truly positive DWI parameters and false positive T2WI ratio and PET-CT)

hyperplasia without atypia was proved in two lesions (Fig. 8). TB was proved in two lesions. Mixed nodal and parenchymal fibrosing sarcoidosis was proved in one lesion (Fig. 9). A complicated cyst without atypia was proved in one lesion.

**The inter-observer agreement or inter-rater reliability**

The inter-observer agreement or inter-rater reliability ranges between good and excellent with the intra-class correlation coefficient (ICC) ranging between 0.85 and 0.94. The results are detailed in Table 1.

**Table 2** Comparative analytic performance of quantitative MRI parameters

P-value	AUC	Cutoff	Sensitivity	Specificity	PPV	NPV
T2WI based L-to-SC SI ratio						
<0.001*	0.860	> 1 <sup>#</sup>	96.4%	80.0%	90%	92.3%
b500-DWI based L-to-SC SI ratio						
<0.001*	0.863	> 0.7 <sup>#</sup>	71.4%	86.7%	90.9%	61.9%
Mean ADC value in 10 <sup>-3</sup> mm <sup>2</sup> /s						
<0.01*	0.77	≤ 1.2 <sup>#</sup>	71.4%	83.3%	84%	70.5%
Minimum ADC value in 10 <sup>-3</sup> mm <sup>2</sup> /s						
<0.001*	0.77	≤ 0.9 <sup>#</sup>	85.7%	66.7%	75.9%	79.2%

L-to-SC SI ratio Lesion-to-spinal cord signal intensity ratio

AUC area under curve, NPV negative predictive value, PPV positive predictive value

\*Statistically significant at p ≤ 0.05

<sup>#</sup> Cutoff value was estimated by Mann–Whitney U and Student-T tests and chosen according to Youden index

**Estimation of the cutoff values according to the Youden index**

The MRI quantitative parameters showed overlap between the pathologically proven benign and malignant lesions; still a significant correlation was proven (P-value ranging from <0.001 to <0.01). The cutoff value for each parameter was then automatically calculated using Mann–Whitney U and Student-T tests according to the Youden index. They are detailed in Table 2.

Further statistical tests of accuracy and ROC analysis were performed as follows.

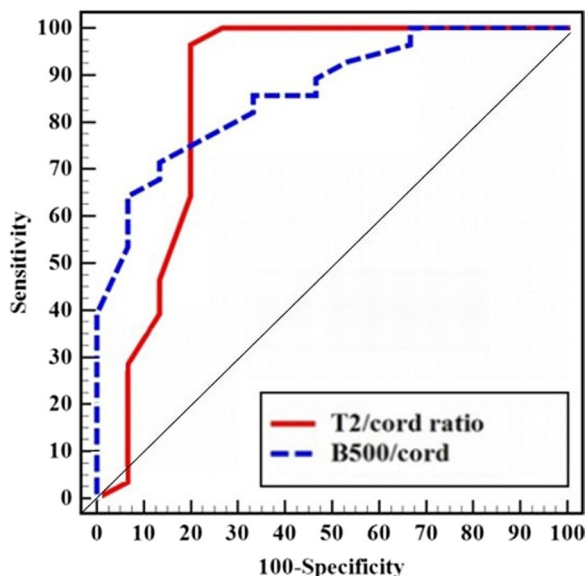


**Fig. 10** ROC curve for T2WI and b500-DWI L-to-cord signal intensity ratios

**T2-WI-MRI lesion-to-spinal cord signal intensity ratio results and statistical analysis**

In T2-WI: The lesion-to-spinal cord signal intensity ratio was higher in the malignant group (1.35 ± 0.29) than in the benign group (0.88 ± 0.40), (P < 0.001). At the estimated cutoff value (> 1), the sensitivity was 96.43% and the specificity was 80.00% in differentiating the benign from the malignant lung lesions with AUC = 0.86. The results are detailed in Table 2 and Fig. 10.

**DWI-MRI lesion-to-spinal cord signal intensity ratio results and statistical analysis**

In b500-DWI: The lesion-to-spinal cord signal intensity ratio was higher in the malignant group (0.70–1.35) than in the benign group (0.20–0.70), (P < 0.001). At the estimated cutoff value > 0.7, the sensitivity was 71.43% and the specificity was 86.67% in differentiating the benign from the malignant lesions with AUC = 0.86. The results are detailed in Table 2 and Fig. 10.

**Mean ADC value results and statistical analysis**

The mean ADC value was lower in the malignant group (0.6–1.3 × 10<sup>-3</sup> mm<sup>2</sup>/s) than the benign group (1–1.6 × 10<sup>-3</sup> mm<sup>2</sup>/s), (P < 0.01). At the estimated cut-off value (≤ 1.2 × 10<sup>-3</sup> mm<sup>2</sup>/s, respectively), the sensitivity was (71.4%) and the specificity was (83.3%), respectively, with AUC = 0.77. The results are detailed in Table 2.

**Minimum ADC results and statistical analysis**

The minimum ADC value was lower in the malignant group (0.3–1.1 × 10<sup>-3</sup> mm<sup>2</sup>/s) than in the benign group (0.7–1.4 × 10<sup>-3</sup> mm<sup>2</sup>/s), (P < 0.001). At the estimated cut-off value (≤ 0.9 × 10<sup>-3</sup> mm<sup>2</sup>/s, respectively), the sensitivity

was (85.7%) and the specificity was (66.7%), respectively, with  $AUC = 0.77$ . The results are detailed in Table 2.

#### **PET-CT results and statistical analysis**

27/28 (96.4%) malignant lesions showed high SUV in PET/CT examination (true positive results) while one carcinoid lesion showed false low SUV (false negative result). On the other hand, 3/15 (20%) benign lesions showed false high SUV (false positive results), including two bronchial hyperplastic lesions without atypia (Fig. 8) and one parenchymal sarcoidosis lesion (Fig. 9). Consequently, the PET/CT accuracy tests' results revealed 96.4% sensitivity and 92.3% specificity for differentiating the malignant from benign lesions with  $AUC = 0.94$ .

#### **Discussion**

Lung cancer is notorious because of its rapid spread and high mortality rates. It is mainly diagnosed by CT and tissue biopsy. It showed variable CT patterns. The diagnosis of malignancy is challenging if the lesion is small or early presenting by the part-solid or ground-glass nodule, and also if it is surrounded by parenchymal lung reaction with consolidation and atelectasis [14]. Similarly, the diagnosis of lung metastatic lesions might be controversial sometimes. Tissue biopsy is not also an option for patients with a bleeding tendency. Here comes the role of MRI and PET/CT evaluation of the suspicious or indeterminate lesions which are defined in the methodology section. The human spinal cord proved to have comparable stable ADC values to be used as a calibrating factor for lesions signal intensity evaluation [15].

This study added to the previous literature a novel quantitative T2WI assessment for the differentiation between malignant and benign lung lesions using lesion-to-spinal cord signal intensity ratio, which proved a high sensitivity equal to the PET/CT with a lower but a good specificity.

This study defined and included the suspicious lung lesions in chest CT examinations. It was quite similar to study of Çakmak et al. [13] which included lung nodules and masses. On the other hand, it was different from the previous studies of Koyama et al. [11], Uto et al. [16], and Guan et al. [17] which focused on the characterization of solitary lung nodules. It was also different from the study of Kolta et al. [18] which expanded its inclusion criteria to involve random benign and malignant lung lesions.

The included number of lesions in this study was 43. It is intermediate between Uto et al. [16], Kolta et al. [18], and Koyama et al. [11] studies which included 28, 30, and 36 lesions, respectively, and Guan et al. [17] as well as Çakmak et al. [13] studies which included 58 and 62 lesions, respectively.

Similar previous research [11, 16–18] presented the quantitative DWI and ADC parameters that could be utilized for the discrimination of malignant and benign lesions including the DWI-based lesion-to-spinal cord signal intensity ratio and minimum ADC value. They all agreed on their acceptable accuracy.

The estimated cutoff value for the DWI-based lesion-to-spinal cord signal intensity ratio in this study was equal to Guan et al. [17] study ( $>0.7$ ) but less than Uto et al. [16] and Kolta et al. [18] studies ( $>1.1$  and  $>1.3$ , respectively).

The sensitivity of the DWI-based lesion-to-spinal cord signal intensity ratio in this study was equal to Guan et al. [17] study (74.1%). On the other hand, its sensitivity in Kolta et al. [18] study was higher (85.7%).

The specificity of the DWI-based lesion-to-spinal cord signal intensity ratio in this study (86.6%) was higher than that estimated by Guan et al. [17] and Kolta et al. [18] (75% each) and slightly lower than that estimated by Koyama et al. [11] (88.9%).

This study is discordant with the Koyama et al. [11] and Uto et al. [16] studies which, respectively, reported low sensitivity and specificity in addition to low AUC of the minimum ADC value for the characterization of malignant lung lesions. This is also totally disagreeing with Guan et al. [17] and Kolta et al. [18] studies as well as Li et al. [19] and Chen et al. [20] large meta-analysis studies which reviewed the literature and reported 88%–80% sensitivity and 89%–93% specificity for using the ADC values for discrimination of malignant from benign lung lesions.

The other advantage also novel in this study was the comparison between the accuracy of specific quantitative MRI parametric tools and the accuracy of PET/CT results in the discrimination of malignant lesions. This fact may justify the low number of included lesions. However, future research on large cohorts of patients is strongly encouraged.

Finally, the discussed MRI quantitative parameters are strongly recommended to be added to any qualitative assessment of chest MRI. The main advantage for the MRI over PET/CT remains the low cost effectiveness and avoidance of irradiation exposure hazards.

The common limitations of chest MRI were encountered in this study including the long time factor of the examination and patients' tolerance as well as the magnetic susceptibility effects of air-filled lung tissue subjected to large magnetic field gradients. Additionally, the cost of a combination between MRI and PET/CT forced many patients to refuse to participate in this study because of economic issues.

## Conclusions

PET-CT remains the most specific and sensitive tool for the differentiation between benign and malignant lesions which are indeterminate in chest CT examinations. The lesion-to-spinal cord signal intensity ratios in T2WI and DWI-MRI and to a minor extent the mean and minimum ADC values are also considered good parameters for this differentiation based on their accurate statistical results, particularly if the PET/CT was not available or feasible. This study added to the previous literature a novel quantitative T2WI assessment which proved a high sensitivity equal to the PET/CT with a lower but a good specificity. The availability, expertise, time factor, and patients' tolerance remain challenging factors for MRI application.

## Abbreviations

DWI	Diffusion-weighted image
MRI	Magnetic resonance imaging
PET	Positron emission tomography
MDCT	Multi-detector computed tomography
ROC	Receiver-operating characteristic
ADC	Apparent diffusion coefficient
ICC	Intra-class correlation coefficient
AUC	Area under curve
L-to-SC SI ratio	Lesion-to-spinal cord signal intensity ratio

## Acknowledgements

Not applicable.

## Author contributions

AS (the corresponding author) is responsible for ensuring that the descriptions are accurate and agreed by all authors. HA, AM, AE, and DA had made substantial contributions to all of the following: (1) The conception and design of the radiological work, (2) The acquisition, analysis and interpretation of radiological data, (3) Drafting the work and revising it. AI had made substantial contribution to; (1) acquisition, analysis and interpretation of clinico-laboratory data, and (2) Drafting the work and revising it. All authors approved the submitted version. All authors have agreed both to be personally accountable for the author's own contributions and to ensure that questions related to the accuracy or integrity of any part of the work, even ones in which the author was not personally involved, are appropriately investigated, resolved, and the resolution documented in the literature. All authors read and approved the final manuscript.

## Funding

No funding was obtained for this study.

## Availability of data and materials

The datasets used and/or analyzed during the current study are available from the corresponding author on reasonable request.

## Declarations

### Ethics approval and consent to participate

The medical ethics were considered and respected. The study was approved by Institutional Ethics Committee in Faculty of Medicine, Alexandria University [IRB No: (00012098), FWA No: (00018699)]. A written informed consent was obtained for all patients.

### Consent for publication

A written informed consent was obtained for all patients.

## Competing interests

The authors declare that they have no competing interests.

## Author details

<sup>1</sup>Department of Radio-Diagnosis, Faculty of Medicine, Alexandria University, Alexandria, Egypt. <sup>2</sup>Master of Radio-Diagnosis and Intervention, Faculty of Medicine, Alexandria University, Alexandria, Egypt. <sup>3</sup>Department of Chest Diseases, Faculty of Medicine, Alexandria University, Alexandria, Egypt.

Received: 16 February 2023 Accepted: 1 April 2023

Published online: 11 April 2023

## References

- Heerink WJ, de Bock GH, de Jonge GJ, Groen HJ, Vliegenthart R, Oudkerk M (2017) Complication rates of CT-guided transthoracic lung biopsy: meta-analysis. *Eur Radiol* 27(1):138–148
- Abehsera M, Valeyre D, Grenier P, Jaillot H, Battesti JP, Brauner MW (2000) Sarcoidosis with pulmonary fibrosis: CT patterns and correlation with pulmonary function. *Am J Roentgenol* 174(6):1751–1757
- Chong S, Lee KS, Chung MJ, Han J, Kwon OJ, Kim TS (2006) Pneumocystosis; comparison of imaging and pathological findings. *Radiographics* 26:59–77
- Falagas ME, Kouranos VD, Athanassa Z, Kopterides P (2010) Tuberculosis and malignancy. *QJM* 103:461–487
- Austin JH, Garg K, Aberle D et al (2013) Radiologic implications of the 2011 classification of adenocarcinoma of the lung. *Radiology* 266(1):62–71
- Pascoe HM, Knipe HC, Pascoe D, Heinze SB (2018) The many faces of lung adenocarcinoma: a pictorial essay. *J Med Imaging Radiat Oncol* 62(5):654–661
- Lococo F, Perotti G, Cardillo G et al (2015) Multicenter comparison of 18F-FDG and 68Ga-DOTA-peptide PET/CT for pulmonary carcinoid. *Clin Nucl Med* 40(3):e183–e189
- Roach DJ, Crémillieux Y, Fleck RJ et al (2016) Ultrashort echo-time magnetic resonance imaging is a sensitive method for the evaluation of early cystic fibrosis lung disease. *Ann Am Thorac Soc* 13(11):1923–1931
- Hatabu H, Ohno Y, Geftter WB et al (2020) Expanding applications of pulmonary MRI in the clinical evaluation of lung disorders: fleischner society position paper. *Radiology* 297(2):286–301
- Wielpütz MO, Lee HY, Koyama H et al (2018) Morphologic characterization of pulmonary nodules with ultrashort TE MRI at 3T. *Am J Roentgenol* 210(6):1216–1225
- Koyama H, Ohno Y, Seki S et al (2015) Value of diffusion-weighted MR imaging using various parameters for assessment and characterization of solitary pulmonary nodules. *Eur J Radiol* 84(3):509–515
- Kim HS, Lee KS, Ohno Y, van Beek EJ, Biederer J (2015) PET/CT versus MRI for diagnosis, staging, and follow-up of lung cancer. *J Magn Reson Imaging* 42(2):247–260
- Çakmak V, Ufuk F, Karabulut N (2017) Diffusion-weighted MRI of pulmonary lesions: comparison of apparent diffusion coefficient and lesion-to-spinal cord signal intensity ratio in lesion characterization. *J Magn Reson Imaging* 45(3):845–854
- Siegel RL, Miller KD, Jemal A (2017) Cancer Statistics, 2017. *CA Cancer J Clin* 67(1):7–30
- Yin Y, Sedlacek O, Muller B et al (2018) Tumor cell load and heterogeneity estimation from Diffusion-weighted MRI calibrated with histological data: an example from lung cancer. *IEEE Trans Med Imaging* 37(1):35–46
- Uto T, Takehara Y, Nakamura Y et al (2009) Higher sensitivity and specificity for diffusion-weighted imaging of malignant lung lesions without apparent diffusion coefficient quantification. *Radiology* 252(1):247–254
- Guan HX, Pan YY, Wang YJ, Tang DZ, Zhou SC, Xia LM (2018) Comparison of various parameters of DWI in distinguishing solitary pulmonary nodules. *Curr Med Sci* 38(5):920–924
- Kolta MF, Abdel-Hamid HM, Hassan BH, Tadros SF (2023) Value of diffusion-weighted MRI and lesion-to-spinal cord signal intensity ratio in pulmonary lesion characterization. *Egypt J Radiol Nuclear Med* 54(1):1–1



19. Li B, Li Q, Chen C, Guan Y, Liu S (2014) A systematic review and meta-analysis of the accuracy of diffusion-weighted MRI in the detection of malignant pulmonary nodules and masses. *Acad Radiol* 21:21–29
20. Chen L, Zhang J, Bao J et al (2013) Meta-analysis of diffusion-weighted MRI in the differential diagnosis of lung lesions. *J Magn Reson Imaging* 37:1351–1358

### **Publisher's Note**

Springer Nature remains neutral with regard to jurisdictional claims in published maps and institutional affiliations.

**Submit your manuscript to a SpringerOpen<sup>®</sup> journal and benefit from:**

- ▶ Convenient online submission
- ▶ Rigorous peer review
- ▶ Open access: articles freely available online
- ▶ High visibility within the field
- ▶ Retaining the copyright to your article

---

Submit your next manuscript at ▶ [springeropen.com](https://www.springeropen.com)

---